Transient Dynamic Analysis of a Head Surrogate Model

A. C. Leung[1], K. E. Simmonds[1], P. Matic[1], J. N. Baucom[1], R. K. Everett[2]

Naval Research Laboratory (Code 6350[1], Code 6303[2])

4555 Overlook Ave, SW

Washington, DC, 20375

Abstract: *A device that can accurately describe the dynamic response of the human head would be a useful tool to understand traumatic brain injuries resulting from blast or blunt force trauma. The Naval Research Laboratory has developed a measurement device (GelMan-Brain) designed specifically to study the dynamic response of the brain from a variety of loading conditions to the human head. The surrogate model of the head is comprised of an anatomically shaped brain with fluid representing cerebral spinal fluid in a skull and surrounded by generalized tissue.*

In this paper, an ABAQUS two dimensional transient modal dynamic finite element analysis was performed of a simplified brain model surrounded by cerebral spinal fluid and encased in PMMA. Viscoelastic material parameters of the brain tissue simulant were obtained from open literature. Low speed loading conditions were applied at different locations of this simple brain model structure. The von Mises stress and pressure contours at different times and displacement history plots are presented. The transient dynamic analyses provide insight into key areas of interest and information on the optimal placement of sensors in a more complex brain surrogate model.

1. Introduction

Explosive devices used on a soldier in the battlefield can cause severe and complicated injuries. Many factors can influence the severity and location of blunt trauma injuries a soldier receives from a blast event. The dispersal pattern and intensity of the blast wave is affected by the shape of weapon and the type of explosives used. The surrounding environment can also change the dynamics of the blast. For example, explosive devices placed in tunnels can focus the direction and intensity of a blast. Also, reverberations and reflection of the blast wave can develop when the explosive device is used inside an enclosed structure. The soldier's position and orientation in relation to the blast wave can also contribute to his physical impairment. Any of these factors can cause complicated injuries in soldiers such as blast lung, hemorrhaging, abdominal injuries, etc. A physician who is tasked with treating many soldiers has the difficulty of quickly and accurately diagnosing their injuries from a multitude of blast scenarios, which may or may not be known. Tools that can be used to measure the dynamic response of the body to blast injuries would be a useful device in the treatment of soldiers. This device could also be applicable to other types of blunt trauma injuries, such as car accidents or sport related injuries.

The Naval Research Laboratory has been developing two measurement tools which can be used to understand body dynamics from blunt trauma: GelMan – Thorax (Figure 1) and GelMan – Brain (Figure 2a).

Figure 1. GelMan – Thorax.

Figure 2. GelMan – Brain (a) three dimensional model (b) two dimensional model

The current GelMan – Thorax is comprised of surrogate tissue that represents heart, lungs and additional organs in a skeletal structure and surrounded by generalized tissue. The GelMan – Brain is comprised of surrogate brain with fluid representing cerebral spinal fluid encased in a skull and surrounded by a generalized tissue. These measurement devices offer a number of advantageous over other types of testing to study blunt or blast trauma injuries. As a manufactured device, GelMan does not have the same ethical concerns as animal or cadaver testing and can be used to provide repeatable results. Refinements to the GelMan – Thorax and GelMan – Brain design are continuously being performed to provide a more representative response to the human body from blunt or blast trauma impacts.

Previous work focused primarily on improving the GelMan – Thorax design using finite element analysis and experimental testing. Surrogate tissue materials development has been an integral part of this program. The individual tissue simulants have been based on various material characterization tests. For example, tests of low velocity impacts on a block of the tissue simulants have been performed to characterize the dynamic response of the different simulants (Leung, 2004; Leung, 2005). The block consisted of standard ordnance gelatin with a cylindrical hole backfilled with different types of simulant materials: the standard ordnance gelatin or modified ordnance gelatin, representing generalized and lung tissue, respectively. The tissue simulant response due to impacts of steel balls with different diameters, masses and impact speeds were measured. The displacements, pressure and resonance peaks obtained from the finite element models compared well to the experimental test results. The computational predictions also provided pressure contours due to ball impacts on tissue simulants.

Experimental field tests have also been performed on the GelMan – Thorax (Simmonds, 2004). It has been deployed to a number of blast test sites to measure human dynamic response in free field and confined environments. For example, one study involved examining the influence of body armor on the thoracic response to free field blasts. The free field blast data indicated that the peak pressures of the lung increased slightly with two types of body armor systems.

The resonance response of the GelMan – Thorax has also been investigated. As with any type of impact loading, when its frequency content is close to the structure's natural frequency, a resonance occurs that amplifies the structure's response. This amplification can inflict the greatest damage to the structure. Understanding the resonance behavior of a structure such as GelMan would provide insight into developing systems to protect against or avoid these types of impact loads. Vibration table tests of the GelMan – Thorax were conducted using a shaker table at the Spacecraft Engineering Division at the Naval Research Laboratory normally used to test the vibrational response of satellites. In the GelMan – Thorax testing, a logarithmic sweep of frequencies was used to identify modal frequencies with constant peak accelerations ranging from 0.25 g to 1 g. Corresponding finite element modal analysis of the GelMan – Thorax was performed and the resonance frequencies compared well to the experiments (Leung, 2006). A parametric analysis was also performed by varying the moduli of the individual tissue simulants by an order of magnitude to determine their influence on the finite element model's modal frequencies.

More recently, NRL has been investigating the use of GelMan – Brain as a device to measure traumatic brain injuries in individuals. Trying to understanding the body response from different types of blast or impact conditions in a three dimensional model would be difficult. Two dimensional models can provide clearer insight into basic brain response from various impact conditions. Complementary experimental models to study the two dimensional effects on the brain from blunt trauma conditions are also being examined (Figure 2b). Two dimensional transient finite element modeling was performed on a simplified brain model surrounded by cerebral spinal fluid and encased in PMMA. These analyses can provide insight into the levels of accuracy required for the development of the geometry, material properties and loading conditions in the more complex three dimensional head so that its dynamic response from a variety of blunt trauma events can be accurately represented.

2. Materials and Methods

The transient response of the two dimensional GelMan – Brain was investigated using computational methods. A description of the geometry, constitutive models, boundary conditions and mesh used in the computational analysis will be discussed in the following sections.

2.1 GelMan – Head Two Dimensional Finite Element Model

2.1.1 Geometry, Boundary Conditions and Material Properties

The finite element mesh of the two dimensional model used for these analyzes contains the following: a simplified brain, cerebral spinal fluid and Polymethylmethacrylate (PMMA) containment (Figure 3).

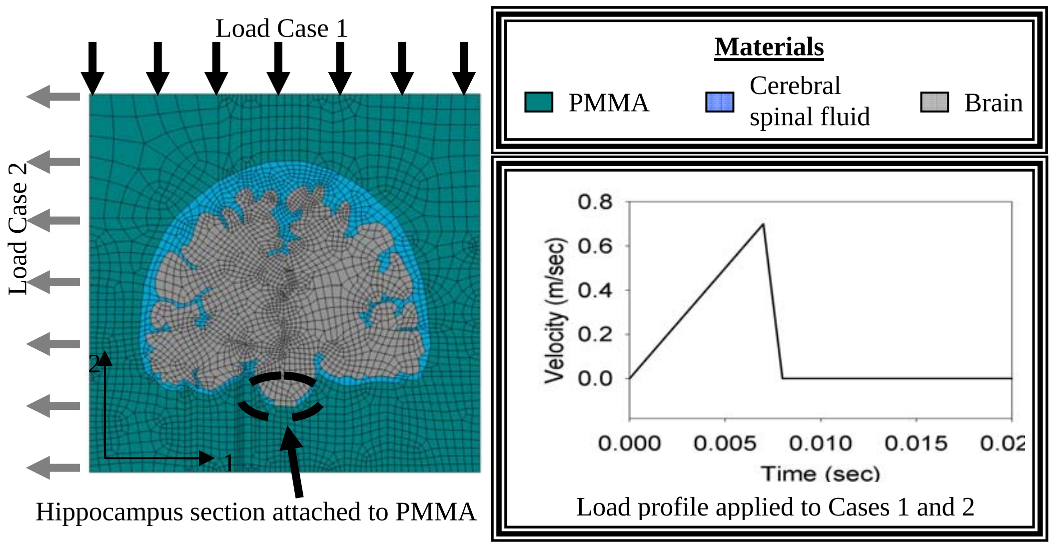

Figure 3. Two dimensional model finite element mesh and loading conditions.

The brain geometry and PMMA cavity size were obtained from a coronal MRI scanned image of the head (Firbank, 2006). The dimensions of the square PMMA used in the simulations were 0.0625 m^2. The brain was attached to the PMMA at the hippocampus to represent the brain's attachment to the brain stem/skull in the human body.

Two types of computational simulations were performed using the finite element model. Loading directions and velocity profile are shown in Figure 3. The velocity loads was applied to the PMMA in the following manner: Case 1 at the top (black arrows) and Case 2 at the side (grey arrows). For both cases, the velocity profile was identical. The velocity increased linearly at a rate of 2 m/sec^2 for 0.007 seconds. Immediately following this time ($t > 0.07$ seconds), the velocity was set to zero to simulate a sudden stop. These loading rates and velocity magnitudes were based approximately on levels used by Willinger (2003).

Material properties for the different components were obtained from open literature. Linear elastic material properties were used for the PMMA material and selected from the Mark (1999). The cerebral spinal fluid behavior was approximated as a low shear, high bulk modulus material using the hyperelastic Neo-Hooke constitutive equation. The brain was modeled as a hyperelastic-viscoelastic material. Material parameters for the cerebral spinal fluid and for the brain were obtained from Ruan (2001) and Miller (1999), respectively.

2.1.2 Finite Element Mesh Description

ABAQUS/Explicit was used to perform a transient dynamic finite element analysis of the two dimensional simplified head model. An explicit analysis was performed for its applicability towards modeling dynamic high speed events. Double precision was used in both simulations to minimize round off-errors. The model was made up of a total of 4360 nodes and 3695 CPE4R elements. This level of mesh density was selected to optimize accuracy of the results while simultaneously minimizing run time.

Linear elastic material properties for the PMMA were incorporated into the ABAQUS input file using the *ELASTIC card. To model the cerebral spinal fluid response, the *HYPERELASTIC, NEO HOOKE card was used for the analysis. The *HYPERELASTIC (N = 1) card in combination with the *VISCOELASTIC (TIME = PRONY) card was used to describe the hyperelastic-viscoelastic brain material. The density was included by the *DENSITY card to account for the inertial effects in these components. Material parameters for the different constitutive models are summarized in Table 1.

The velocity loading condition was applied using the *AMPLITUDE card in combination with the *BOUNDARY card. The total simulation time was set to 0.2 seconds in order to accurately observe the response of the brain following the high speed dynamic loading conditions. The *OUTPUT command was used with the VARIABLE = PRESELECT option to obtain both field and history data. The data collection time for the *OUTPUT, FIELD option was set to 0.00025 seconds while the data collection frequency for the *OUTPUT, HISTORY option was set to 2000 intervals. These intervals were deemed sufficient to capture the structural response of this model.

Table 1: Material properties of two dimensional model

<table>
<tr><th>Material</th><th>Density (kg/m^3)</th><th colspan="2">Elastic Modulus (Pa)</th><th colspan="2">Poisson’s Ratio</th></tr>
<tr><td>PMMA</td><td>1190.0</td><td colspan="2">3.1×10^9</td><td colspan="2">0.3</td></tr>
<tr><td colspan="2"></td><td colspan="2">Bulk Modulus (Pa)</td><td colspan="2">Shear Modulus (Pa)</td></tr>
<tr><td>Cerebral spinal fluid</td><td>1040.0</td><td colspan="2">0.0219×10^9</td><td colspan="2">5×10^5</td></tr>
<tr><td colspan="2" rowspan="2"></td><td colspan="2">Hyperelastic Parameters</td><td colspan="2">Viscoelastic Parameters</td></tr>
<tr><td>Bulk Modulus (Pa)</td><td>Instantaneous response (Pa)</td><td colspan="2">Characteristic time</td></tr>
<tr><td>Brain</td><td>1046.0</td><td>2.19×10^9</td><td>$C_{100} = 263$
$C_{010} = 263$</td><td>t_1=0.5 seconds
g_1 =0.450</td><td>t_2=50 seconds
g_2=0.365</td></tr>
</table>

3. Results and Discussion

The finite element transient analysis was performed on a two dimensional model of the brain, cerebral spinal fluid and PMMA containment. Stable time increments for both simulations were approximately 1.82×10^{-7} sec. The computational models completed in approximately 8 CPU hours using 15 GB of memory.

Figures 4-8 show the von Mises stress contours in the brain at increasing times for the two different loading conditions. At the beginning of the simulation (time = 0.001 seconds), stresses appear: at the superficial medial brain section in Case 1 and at the superior brain section in Case 2. The stresses overall then decrease as the velocity increases (Figure 5) and once the velocity loading condition is set to zero, the von Mises stresses increases rapidly in both cases (Figure 6). At this time, the highest von Mises stresses are observed in Case 1 is at the superficial medial and superficial lateral brain sections while Case 2 it is all along the superior brain except at the left lateral section. Note for both cases, the von Mises stress is high at the narrow region immediately above the hippocampus. These higher stresses are caused by the oscillations of the gyri in the direction of travel. Case 2 experiences additional stresses caused by the brain pivoting about the hippocampus. The stresses reaches a peak for both cases at time = 0.00925 seconds (Figure 7). Maximum von Mises stresses of 656 Pa and 614 Pa for both Case 1 and Case 2, respectively, are located at superficial medial brain section. High stresses are observed primarily along the brain superior as opposed to the brain inferior. At time = 0.049 seconds (Figure 8), the stresses overall have decreased. High stresses are mostly observed at the superficial medial brain section for Case 1 and near the narrower section of the hippocampus in both cases. From these stress contour plots, the following general observations can be made: 1. stresses are typically higher along the superior brain as opposed to the inferior and 2. as a result of gyri oscillations from the application of the loading velocity conditions, high stress concentrations typical occur at the seluci.

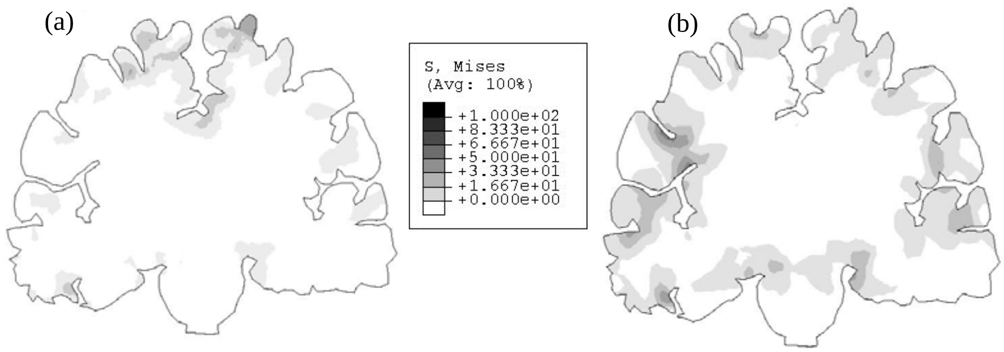

Figure 4: Von Mises stress contours at time = 0.001 seconds for (a) Case 1: motion in the 2-direction (b) Case 2: motion in the 1-direction

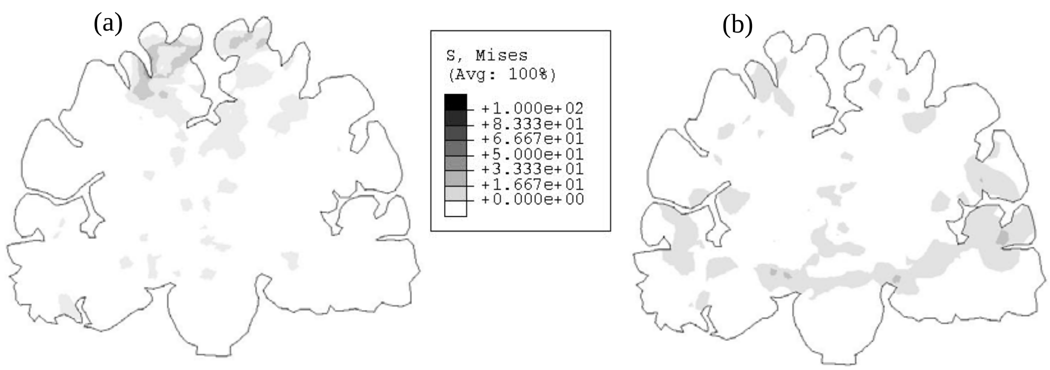

Figure 5: Von Mises stress contours at time = 0.0035 seconds for (a) Case 1: motion in the 2-direction (b) Case 2: motion in the 1-direction

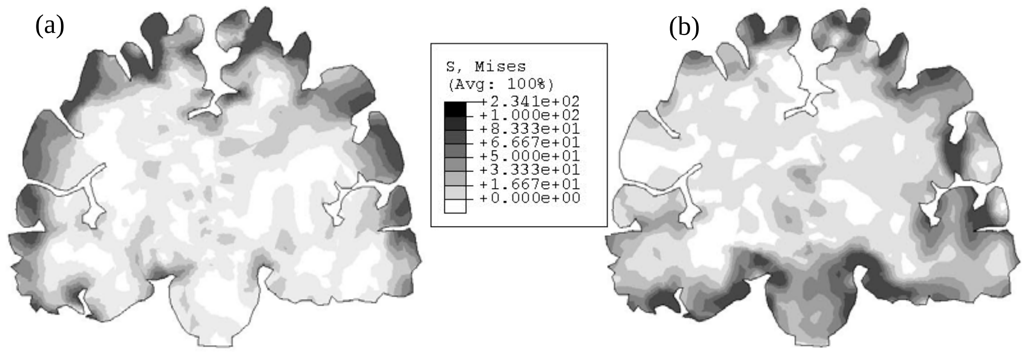

Figure 6: Von Mises stress contours at time = 0.0075 seconds for (a) Case 1: motion in the 2-direction (b) Case 2: motion in the 1-direction

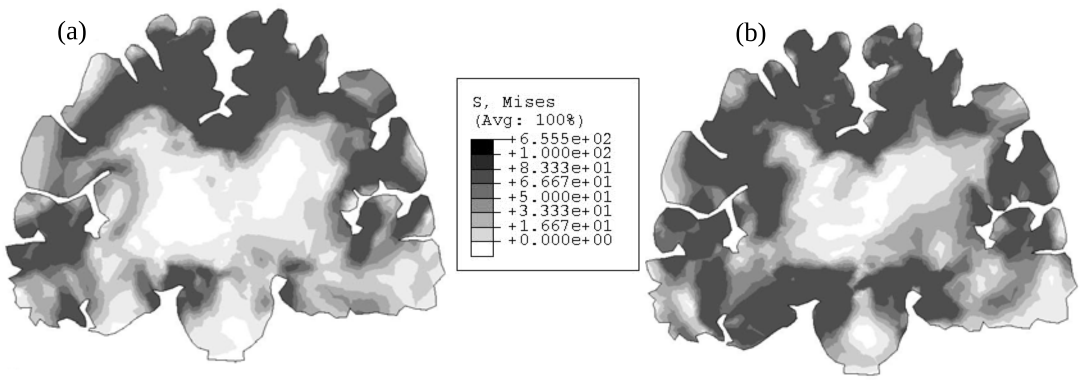

Figure 7: Von Mises stress contours at time = 0.00925 seconds for (a) Case 1: motion in the 2-direction (b) Case 2: motion in the 1-direction

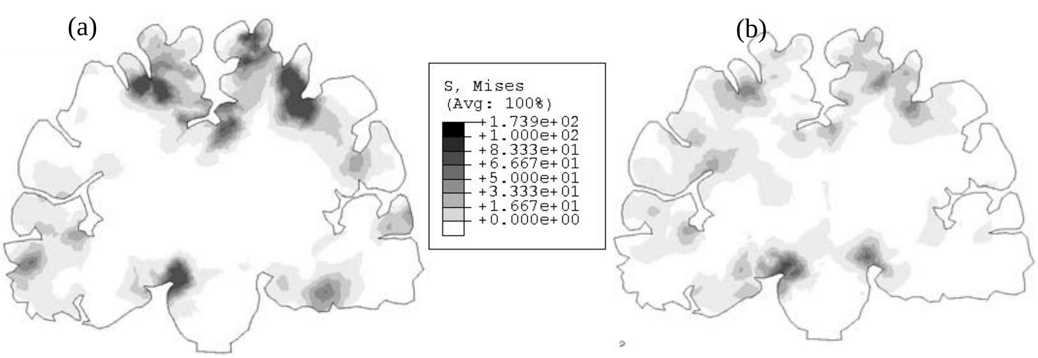

Figure 8: Von Mises stress contours at time = 0.049 seconds for (a) Case 1: motion in the 2-direction (b) Case 2: motion in the 1-direction

Pressure contours are shown in Figures 9-12 for the different loading conditions. Positive (compressive) pressure to negative (tensile) pressure is observed in the direction of motion at time = 0.00025 seconds for both cases. Immediately after the velocity is set to zero (Figures 10 and 11), positive pressure and negative pressure become more pronounced in both cases and the pressures oscillate as the simulation progresses. The dichotomy of pressure is from the oscillations of the brain in the direction of motion. Antisymmetric pressure contours are also occasionally observed in Case 2 such as at time = 0.0125 seconds. This is a result of the pivoting motion of the brain around the hippocampus.

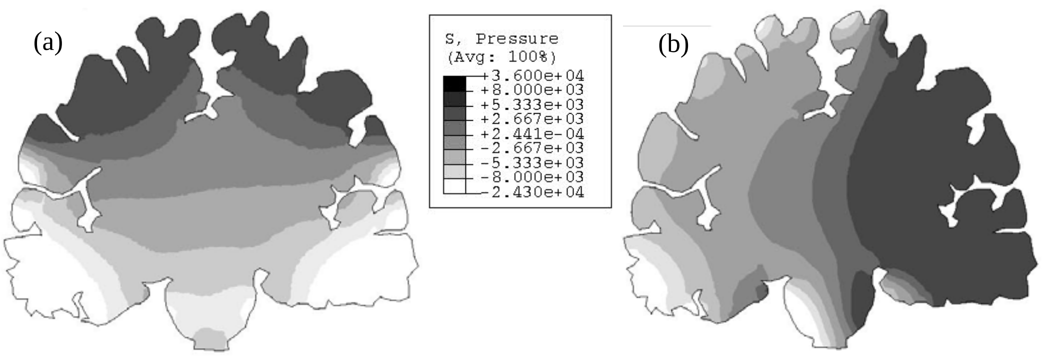

Figure 9: Pressure stress contours at time = 0.00025 seconds for (a) Case 1: motion in the 2-direction (b) Case 2: motion in the 1-direction

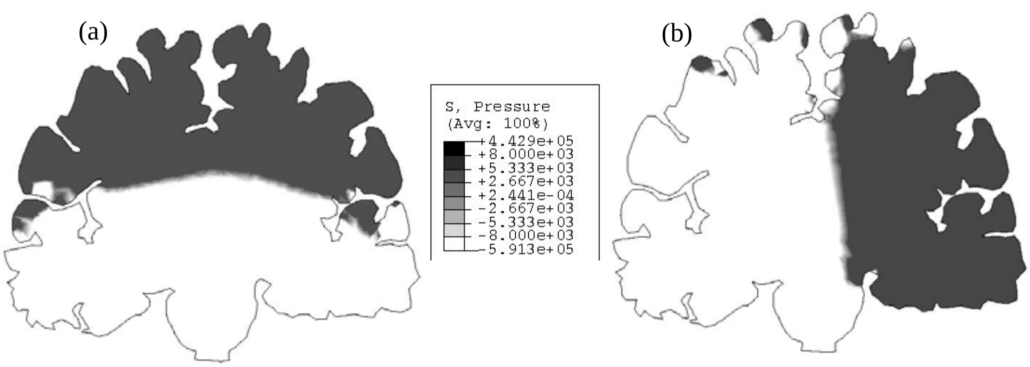

Figure 10: Pressure stress contours at time = 0.0085 seconds for (a) Case 1: motion in the 2-direction (b) Case 2: motion in the 1-direction

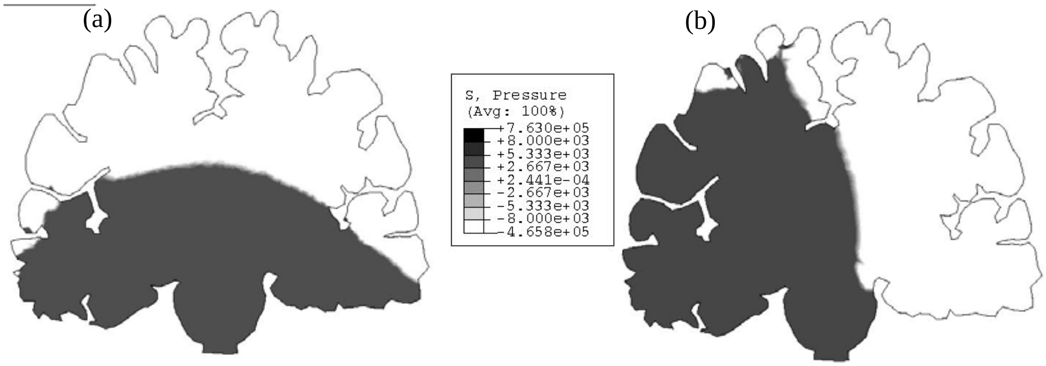

Figure 11: Pressure stress contours at time = 0.0095 seconds for (a) Case 1: motion in the 2-direction (b) Case 2: motion in the 1-direction

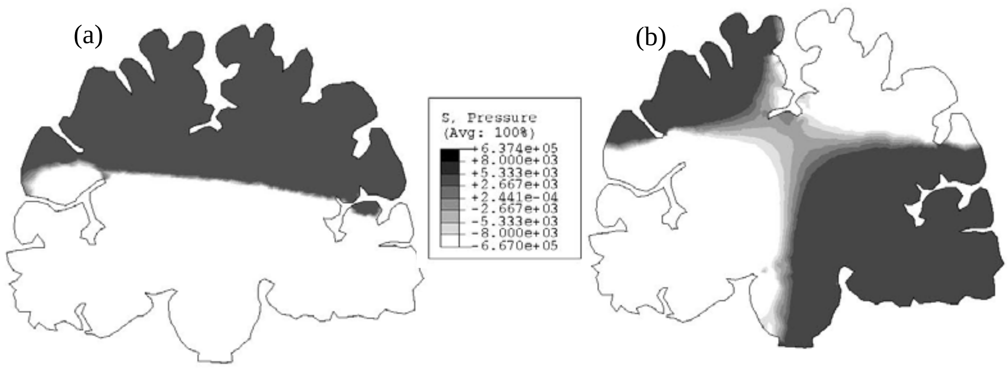

Figure 12: Pressure stress contours at time = 0.0125 seconds for (a) Case 1: motion in the 2-direction (b) Case 2: motion in the 1-direction

Time versus displacement component (U_1 and U_2) history plots at two lateral superior points in the brain are presented in Figures 13-14 to show its response after the velocity loading condition has been set to zero. Note the ranges of the U_1 and U_2 displacement axes in these figures are different so that the response can be more easily observed. For both cases, the displacement components decrease to less than 98% of the maximum by time = 0.05 seconds. The loading velocity direction causes a higher peak to peak displacement in the respective components, i.e. peak to peak U_2 (U_1) displacement is higher in Case 1 (Case 2). The U_1 displacement decreases quickly after 0.001 sec as the connection of the brain to the Plexiglas constrains the motion in that direction. Also, in phase and 180° out of phase oscillations are observed when comparing the displacements components at the different locations. For example, in Case 1, the U_1 displacements of Figure 13a are 180° out of phase with one another while the U_2 displacements of Figure 13b are in phase with one another.

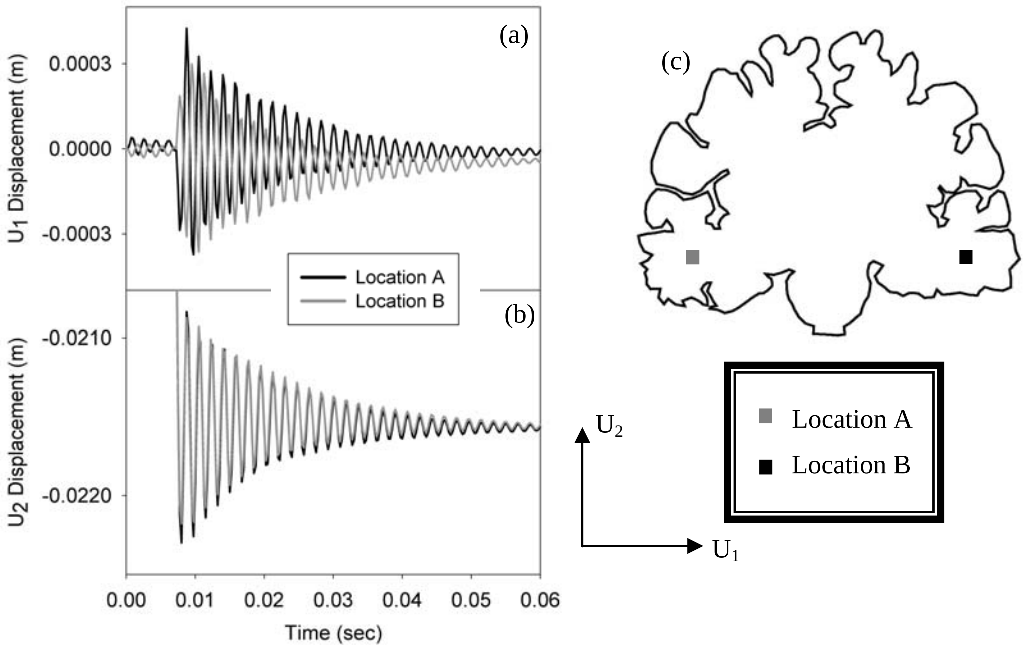

Figure 13: Time history plots for Case 1 (a) displacement in the 1-direction (U_1), (b) displacement in the 2-direction (U_2), (c) locations of displacement measurement in brain.

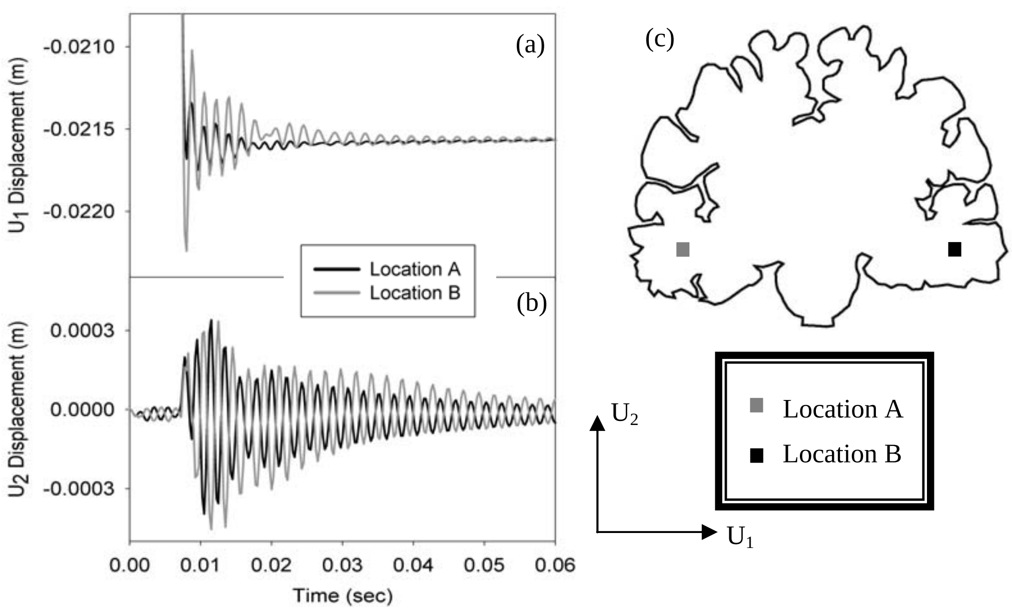

Figure 14: Time history plots for Case 2 (a) displacement in the 1-direction (U_1), (b) displacement in the 2-direction (U_2), (c) locations of displacement measurement in brain.

Based on these simulations, a preliminary assessment of optimal sensor placement may be made for these types of loading conditions. Stress measurement sensors may best be placed near the gyri of the brain surrogate as regions of high von Mises stress typically occur there. It may also be important to place sensors in the area near the model's hippocampus to observe the pivoting motion. The incorporation of pressure sensors into the GelMan – Brain may be useful in observing the oscillating tensile and compressive pressures.

4. Conclusions

A two dimensional transient finite element analysis of the brain was performed using ABAQUS/Explicit. Von Mises stress and pressure contour distributions presented show the areas of interest. The different loading conditions show distinct differences in the structural response of the brain. The inclusion of the brain ridges into the model influences the structural response of the models for these different types of loading conditions. Connecting the brain to the PMMA at the hippocampus has also shown to affect the dynamic response of the system. For these loading cases, a preliminary assessment for optimal placement of sensor has been made.

To provide insight into the development of a better surrogate human measurement tool, future work will include: 1. extending the current analyzes of the two dimensional finite element brain model and 2. developing a three dimensional finite element model of the head. Various material characterization tests (i.e., Instron, dynamic mechanical analysis, etc.) of the surrogate brain material and fluid representing cerebral spinal fluid that will be used in the experimental models will be performed. Future analysis on the two dimensional finite element models will include the following to determine how material properties can influence the dynamic response in the brain: 1. use of the brain simulant tissue and fluid representing cerebral spinal fluid, 2. a parametric study of the damping coefficient into the cerebral spinal fluid and 3. the inclusion of white matter in the brain. Steady-state dynamic analyses on the two dimensional model will also provide a better assessment of the optimal sensor placement. The results of these future two dimensional and three dimensional analyzes will be continuously compared to corresponding experimental tests.

5. References

1. ABAQUS User's Manual Ver.6.6, (2006). ABAQUS, Inc., Pawtucket, Rhode Island.
2. Firbank, M., "MRI Scan with Hippocampus Indicated", 31 May 2006 5 February 2007 http://commons.wikimedia.org/wiki/Image:Hippocampus-mri.jpg.
3. Leung, A.C., Simmonds, K.E., Chase, M., Geltmacher, A.B., "Finite Element Modeling of the Impact Loading on Tissue Simulants", *Proceedings of 2004 ABAQUS Conference*, May 25-27, 2004, Boston, MA.
4. Leung, A.C., Simmonds, K.E., Geltmacher, A.B., "Dynamic/ Mechanical Characterization Of Simulant Human Tissue Under Impact Loading Conditions", International Symposium on Plasticity 2005, Kauai, Hawaii, January 3-8, 2005.

5. Leung, A.C., Simmonds, K.E., Matic, P., Geltmacher, A.B., “Surrogate Human Thorax Modal Frequency Response”, *Proceedings of 2006 ABAQUS Conference*, May 23-25, 2006, Boston, MA.
6. Mark, J., ed. Polymer Data Handbook, Oxford University Press, New York, 1999.
7. Miller, K., “Constitutive model of brain tissue suitable for finite element analysis of surgical procedures”, Journal of Biomechanics, Vol. 32, 1999, pp. 531-537.
8. Ruan, J.S., Zhou, C., Khalil, King, A. “Techniques and Applications of Finite Element Analysis of the Biomechanical Response of the Human Head to Impact”, *CRC Press LLC*, 2001.
9. Simmonds, K.E., Matic, P., Chase, M., Leung, A.C., “GelMan: A Physical Model for Measuring the Response to Blast”, NRL Review 2004, pp. 156-158.
10. Willinger, R., Baumgartner, D. “Numerical and physical modeling of the human head under impact-towards new injury criteria”, International Journal of Vehicle Design, Vol 32, No. ½, 2003, pp. 94-115.